U.S. DEPARTMENT OF ENERGY | Office of Science

DOE/SC-ARM-TR-205

Vertically Resolved Retrievals of Aerosol Concentrations and Effective Radii from the DOE Combined HSRL and Raman lidar Measurement Study (CHARMS) Merged High-Spectral-Resolution Lidar-Raman Lidar Data Set

R Ferrare
M Clayton
E Chemyakin
J Goldsmith
R Kuehn
W Marais
T Thorsen
D Muller
S Burton
R Holz
E Eloranta
R Newsom

January 2017

ARM
CLIMATE RESEARCH FACILITY

DISCLAIMER

DOE/SC-ARM-TR-205

Vertically Resolved Retrievals of Aerosol Concentrations and Effective Radii from the DOE Combined HSRL and Raman lidar Measurement Study (CHARMS) Merged High-Spectral-Resolution Lidar-Raman Lidar Data Set

R Ferrare, National Aeronautics and Space Administration
Principal Investigator

T Thorsen, National Aeronautics and Space Administration
M Clayton, Science Systems and Applications, Inc.
D Muller, Science Systems and Applications, Inc.
E Chemyakin, Science Systems and Applications, Inc.
S Burton, National Aeronautics and Space Administration
J Goldsmith, Sandia National Laboratories
R Holz, University of Wisconsin, Madison
R Kuehn, University of Wisconsin, Madison
E Eloranta, University of Wisconsin, Madison
W Marais, University of Wisconsin, Madison
R Newsom, Pacific Northwest National Laboratory
Co-Investigators

January 2017

Work supported by the U.S. Department of Energy,
Office of Science, Office of Biological and Environmental Research

Acronyms and Abbreviations

AA	Arrange and Average (algorithm)
ACE	Aerosol-Clouds-Ecosystem (mission)
AERI	Atmospheric Emitted Radiance Interferometer
AERONET	AErosol RObotic NETwork
ALIVE	Aerosol Lidar Validation Experiment
AOT	Aerosol Optical Thickness
ARM	Atmospheric Radiation Measurement (Climate Research Facility)
BNL	Brookhaven National Laboratory
CHARMS	Combined HSRL and Raman lidar Measurement Study
DISCOVER-AQ	Deriving Information on Surface conditions from Column and Vertically Resolved Observations Relevant to Air Quality
ENA	Eastern North Atlantic
FEX	feature detection and extinction
FOV	field of view
G-1	Gulfstream-1
GSFC	Goddard Space Flight Center (NASA)
HSRL	High-Spectral-Resolution Lidar
IR	infrared
LaRC	Langley Research Center (NASA)
NASA	National Aeronautics and Space Administration
NSA	North Slope of Alaska
OE	Optimal Estimation
PI	Principal Investigator
RLID	Raman lidar
RMS	root mean square
SDA	spectral deconvolution method
SGP	Southern Great Plains
SNR	signal-to-noise ratio
SSEC	Space Science and Engineering Center (UW)
TCAP	Two-Column Aerosol Project
TiARA	Tikhonov Advanced Regularization Algorithm
UT	Universal Time
UW	University of Wisconsin

Contents

Acronyms and Abbreviations iii
1.0 Introduction 5
2.0 Instruments 6
2.1 Raman Lidar (RLID) 6
2.2 UW HSRL 6
3.0 Data Processing 7
3.1 HSRL Data Processing 8
3.2 Initial Data Processing and Data Quality Review 8
3.3 Calibration of the 1064 nm Aerosol Backscatter Profiles 10
4.0 Aerosol Microphysical Retrievals 12
5.0 Aerosol Microphysical Retrieval Comparisons with AERONET 17
6.0 Summary and Outlook 24
7.0 References 25

Figures

1 Daily and column-average CHARMS lidar aerosol extensive and intensive parameters for the entire CHARMS period. 9
2 Same as for Figure 1 except for a subset of days that use 1064 nm aerosol backscatter profiles computed using the revised calibration method. 11
3 Example “3β+2α” data set for September 6, 2015. 12
4 TiARA retrieval results for September 5, 2015. 14
5 Same as Figure 4 except for AA+TiARA retrieval results. 16
6 Comparison of TiARA aerosol retrieval results derived using NASA LaRC airborne HSRL measurements and airborne in situ data collected over the Houston, Texas region during the NASA DISCOVER-AQ mission. 17
7 Comparison of aerosol optical depth derived from the CHARMS measurments and AERONET data. 18
8 Comparison of fine- and coarse-mode AOD and fine-mode fraction from TiARA and AERONET SDA retrievals. 19
9 Same as Figure 8 except comparison of fine- and coarse-mode AOD and fine-mode fraction from AA+TiARA and AERONET SDA retrievals. 20
10 Comparison of fine and total volume concentrations from TiARA and AERONET retrievals. 21
11 Same as Figure 10 except for comparison of fine and total volume concentrations from AA+TiARA and AERONET retrievals. 22
12 Comparison of fine and total effective radii from TiARA and AERONET retrievals. 23
13 Same as Figure 12 except for comparison of fine and total effective radii from AA+TiARA and AERONET retrievals. 23

1.0 Introduction

The Department of Energy's (DOE) Atmospheric Radiation Measurement (ARM) Climate Research Facility is a key component of DOE's research strategy to address global climate change. The objective of the ARM Facility is to provide an experimental testbed for studying important atmospheric effects, particularly cloud and aerosol processes, and testing parameterizations of these processes for use in climate change models. ARM observational sites include a broad array of instruments to characterize cloud and aerosol properties, atmospheric state variables, and incoming and outgoing radiation. Advanced lidar systems provide valuable and unique information about the atmospheric column. We examine the potential for providing vertically resolved information about aerosol size and concentration with a combination of two such lidar systems, the Raman lidar and the High-Spectral-Resolution Lidar (HSRL).

Currently ARM has a limited ability to remotely measure profiles of aerosol optical and microphysical properties on an operational basis. Although the Southern Great Plains (SGP), Eastern North Atlantic (ENA), and North Slope of Alaska (NSA, Oliktok Point location only) Raman lidars provide profiles of aerosol backscatter and extinction at 355 nm, additional information is required to better characterize the impacts of aerosols on radiation and clouds. Recent advances in lidar retrieval theory and algorithm development (Müller et al. 1999, 2014; Chemyakin et al. 2014) demonstrate that multi-wavelength lidar retrieval algorithms that use measurements of aerosol extinction at both 355 and 532 nm and backscatter at 355, 532, and 1064 nm have the potential to constrain both the aerosol optical (e.g., complex index of refraction, scattering, etc.) and microphysical properties (e.g., effective radius, concentration). This advancement greatly increases the utility of the remote-sensed aerosol observations. Based on this work, the HSRL group at the National Aeronautics and Space Administration (NASA)'s Langley Research Center (LaRC) developed automated algorithms for retrieving aerosol optical and microphysical properties, demonstrated these retrievals using data from the unique NASA/LaRC airborne multi-wavelength HSRL-2 system, and validated these retrievals using coincident airborne in situ data (Müller et al. 2014; Sawamura et al. 2017).

We report here on the use of ARM instrumentation to gather a multi-wavelength ground-based lidar data set to test such retrievals. Continuous (24/7) operation of the co-located SGP Raman lidar and University of Wisconsin (UW) HSRL during the 10-week Combined HSRL and Raman lidar Measurement Study (CHARMS) (mid-July through September 2015) allowed the acquisition of a unique, multi-wavelength ground-based lidar data set. The ARM SGP Raman lidar (RLID) measured profiles of aerosol backscatter, extinction, and depolarization at 355 nm and profiles of water vapor mixing ratio and temperature. The UW HSRL simultaneously measured profiles of aerosol backscatter, extinction and depolarization at 532 nm and aerosol backscatter at 1064 nm. This RLID+HSRL combination provided a test data set to investigate these more advanced aerosol retrieval techniques with the potential to greatly improve aerosol characterization in the lower atmosphere.

2.0 Instruments

2.1 Raman Lidar (RLID)

The RLID was designed for the ARM Facility to measure water vapor throughout the lower troposphere across the diurnal cycle in an automated manner (Goldsmith et al. 1998). It transmits nominally 350 mJ pulses of 355 nm laser energy into the atmosphere at 30 Hz, and measures the elastic backscatter at the laser wavelength and the rotational/vibrational Raman-shifted backscatter from nitrogen and water vapor molecules at 387 and 408 nm, respectively. The ratio of the signal in the 408 to 387 nm channels, after some corrections to account for instrumental features, is proportional to the water vapor mixing ratio (Turner and Goldsmith 1999). Water vapor mixing ratio profiles are computed using the ratio of the Raman water vapor signal to the Raman nitrogen signal. Relative humidity profiles are computed using these profiles and the temperature profiles from a collocated Atmospheric Emitted Radiance Interferometer (AERI).

Profiles of aerosol scattering ratio (355 nm) are derived using the Raman nitrogen signal and the elastic signal. Aerosol volume backscattering cross-section profiles (355 nm) are then computed using the aerosol scattering ratio and molecular scattering cross-section profiles derived from atmospheric density data. Aerosol extinction (355 nm) profiles are computed from the derivative of the logarithm of the Raman nitrogen signal with respect to range and then accounting for the contribution from molecular scattering. Aerosol Optical Thickness (AOT) is derived by integration of the aerosol extinction profile with altitude. During the Aerosol Lidar Validation Experiment (ALIVE) the Raman lidar demonstrated that it can measure (355 nm) extinction profiles with systematic uncertainties not exceeding the range of 15-20%, or 0.025 km (whichever is larger) (Schmid et al. 2009). The copolarized and cross-polarized signals (with respect to the laser beam's polarization) are also measured at the laser wavelength. These signals are used to derive the linear depolarization, which is defined as the ratio of the backscattered signals that are polarized orthogonal and parallel to the linearly polarized outgoing laser beam.

Profiles of water vapor mixing ratio, relative humidity, aerosol backscattering, and aerosol extinction are derived routinely using a set of automated algorithms (Turner et al. 2002). Recently, a comprehensive set of algorithms was developed that derive aerosol and cloud features, provide an improved cloud mask, and derive profiles of aerosol and cloud backscatter and extinction (355 nm) (Thorsen et al. 2015; Thorsen and Fu 2015). We use these algorithms to process both the Raman lidar and HSRL aerosol backscatter and extinction profiles in order to have a consistent set of profiles, with equivalent resolutions and averaging, across all wavelengths.

2.2 UW HSRL

The UW bagoHSRL, named after the UW-Space Science and Engineering Center (SSEC) Winnebago mobile measurement platform, was developed to serve as an autonomous lidar for use in a mobile trailer equipped with other instruments. This HSRL operates at eye-safe levels in the transmitted beam and is designed to operate with low maintenance. The lidar measures aerosol backscatter profiles at both 532 and 1064 nm, and aerosol extinction profiles at 532 nm, using the HSRL technique (Grund and Eloranta 1991; Piironen and Eloranta 1994) (see also https://ams.confex.com/ams/95Annual/webprogram/Paper259645.html). The bagoHSRL system deployed

for CHARMS included a two-field-of-view (FOV) optical detection system in order to measure molecular backscatter and hence aerosol extinction for altitudes within a kilometer above the surface and for altitudes consistent with the RLID measurements. The bagoHSRL also measured aerosol depolarization at 532 nm.

3.0 Data Processing

CHARMS data were collected from July 18 through September 30, 2015 when the UW HSRL was deployed at the SGP site. The processing of both data sets used a series of algorithms developed initially for processing the Raman lidar data (Thorsen et al., 2015; Thorsen and Fu 2015) These algorithms, which were developed to optimize the retrievals of aerosol extinction and feature detection for the Raman lidar, make use of various retrieval algorithms for various channels that are then combined into a single best estimate based on the signal-to-noise ratio (SNR) and accuracy of each channel's calibration and overlap function.

Details of the Raman lidar processing for aerosol backscattering and extinction are provided in Thorsen and Fu (2015). Aerosol backscatter profiles are computed from the aerosol scattering ratio profiles derived from the ratio of signals from the elastic and nitrogen signals for both the high-altitude (i.e., narrow-field-of-view) and the low-altitude (i.e., wide-field-of-view) channels. In the originally developed feature detection and extinction (FEX) algorithm (Thorsen and Fu 2015), the low-altitude channels were used when the SNR in those channels was greater than 10. An examination of the CHARMS data showed this requirement to be unnecessarily restrictive, causing a heavy reliance on the noisier low-altitude-channel values. In the revised version used to process the CHARMS data, in addition to this requirement, the low-channel data were only used below 0.8 km.

The FEX algorithm retrieves a smoothed lidar ratio profile by smoothing both the backscatter and extinction coefficients using a two-dimensional Gaussian weight. In order to avoid potentially large biases introduced by uncertainties in the overlap function, the original algorithm avoided using high-channel data below 1.5 km and low-channel data below 0.5 km. In this revised version, the cutoff height for the high-channel data was raised to 2 km to help further reduce problems associated with uncertainties in the overlap function.

The lidar ratios in the original FEX algorithm were derived from the low- and high-channel data and were averaged in order to reduce random errors below 30%. In the revised algorithm, the maximum lidar ratio uncertainty in the high channels was reduced to 15% to reduce the random errors in the input parameters for the microphysical retrievals. The maximum lidar ratio uncertainty in the low channels was kept at 30%. Reducing the uncertainty to lower values forced the algorithm to use high-channel data in regions where uncertainty in the overlap function correction produced unacceptably large systematic uncertainties in the derived lidar ratios.

After deriving smoothed lidar ratio profiles, the FEX algorithm retrieves quasi-high-resolution profiles of aerosol extinction by multiplying the smoothed lidar ratio profiles by the unsmoothed particulate backscatter coefficient profiles. This produces extinction and backscatter profiles with similar resolutions. Initial processing of the HSRL data by personnel at UW produced profiles of aerosol backscatter (532 and 1064 nm), aerosol extinction, and aerosol depolarization (532 nm) (Eloranta 2014).

3.1 HSRL Data Processing

The HSRL data were processed in a similar manner as the Raman lidar data to match the times, altitudes, and temporal and vertical resolutions of the Raman lidar data. The 532 nm molecular signal from HSRL is used to obtain profiles of smoothed lidar ratio and aerosol extinction (532 nm). Although the HSRL does not employ separate low- and high-sensitivity channels like the Raman lidar, the processing and averaging of the HSRL data were done to mimic the processing of the Raman lidar low- and high-sensitivity channels for consistency. Smoothed profiles of the 532 nm lidar ratio were computed from the aerosol HSRL backscatter and extinction profiles in the same manner as were the low- and high-sensitivity lidar ratio profiles from the Raman lidar. These HSRL "low" and "high" (532 nm) lidar ratio profiles were then combined in the same manner as those derived at 355 nm from Raman lidar low and high lidar ratio profiles. The 532 nm extinction profiles were then computed as the product of the 532 nm lidar ratio and 532 nm aerosol backscatter profiles.

The resulting netCDF data files contain several parameters associated with the computations described above. Typically these parameters correspond to the low, high, and combined channels. For example, there are profiles called "rl_extinction_e_n2_low", "rl_extinction_e_n2", and "rl_extinction_be". In this case, the first parameter corresponds to the aerosol extinction (355 nm) computed from the Raman lidar low channel, the second parameter corresponds to the aerosol extinction (355 nm) computed from the Raman lidar high channel, and the third parameter corresponds to the aerosol extinction (355 nm) computed by combining the results from the two channels.

3.2 Initial Data Processing and Data Quality Review

Diagnostic plots were constructed to assess the quality of the initial data processing before attempting to use the results in the aerosol microphysical retrieval algorithms.

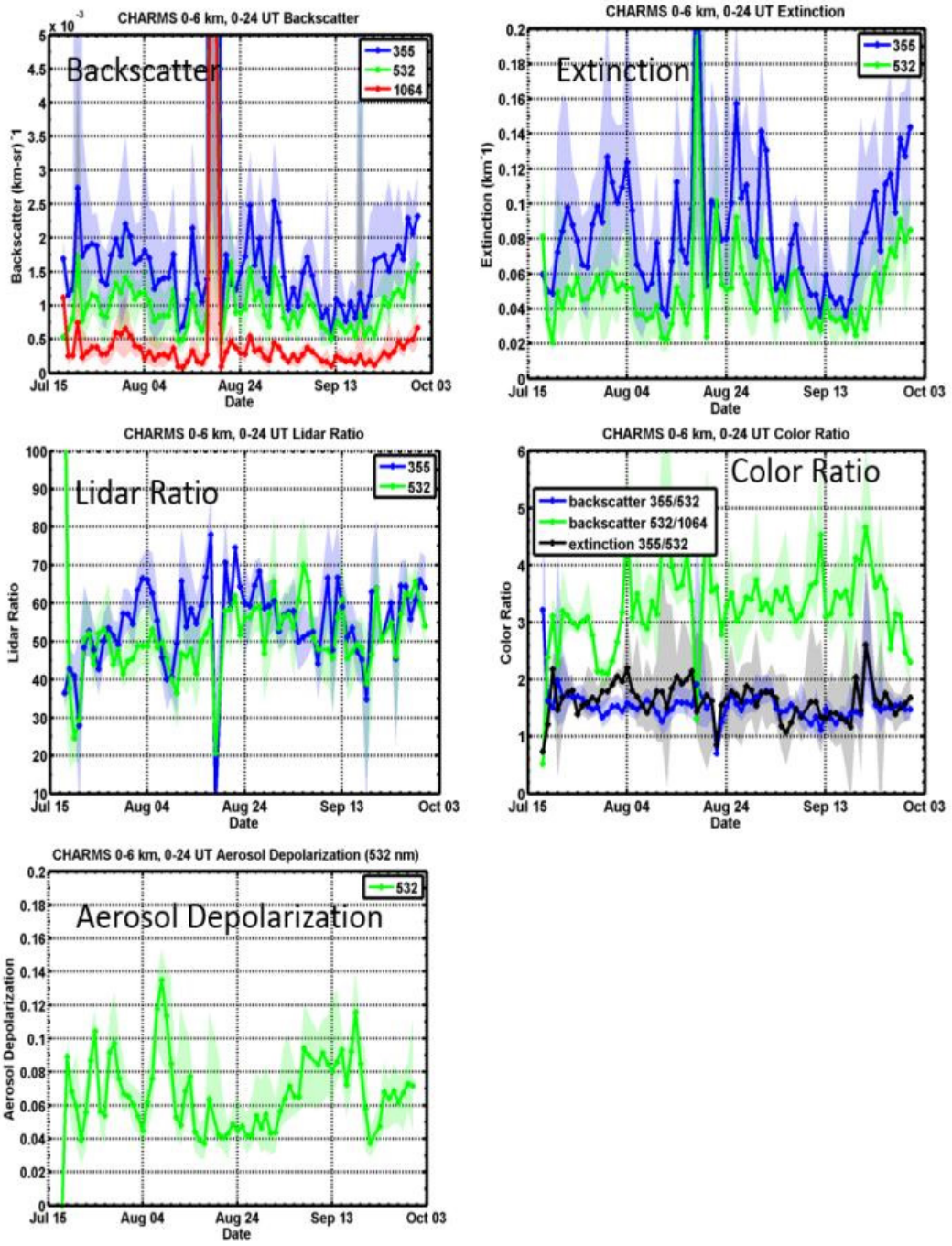

Figure 1. Daily and column-average CHARMS lidar aerosol extensive (extinction, backscatter) and intensive (lidar ratio, color ratio, aerosol depolarization) parameters for the entire CHARMS period. These use results from the initial 1064 nm aerosol backscatter profiles.

Figure 1 shows aerosol extensive (backscattering and extinction) and intensive (backscatter and extinction color ratios, lidar ratios, depolarization ratios) parameters. Median values (solid lines) and the 10th-90th percentile values (shaded areas) are shown for relevant variables from the CHARMS data sets for each day. All values for each day were used, excluding altitudes above 6 km, extinction (355 and 532) below 0.01 km-1, and data classified as clouds. The values of nearly all aerosol parameters shown are consistent

with values of the aerosol extensive and intensive parameters measured by the NASA LaRC airborne HSRL-1 and HSRL-2 systems (Burton et al. 2012). However, with the exception of a few days at the end of July and the beginning of August, the aerosol backscatter color ratio values (532/1064 nm) were significantly higher than those measured by the airborne HSRL systems. The airborne HSRL measurements, as well as other measurements and modeling studies, show that the backscatter color ratios (532/1064) were typically less than 2 and almost always below 3. However, as shown in Figure 1, the 532/1064 backscatter color ratios computed from the initial CHARMS data were usually greater than 3. This behavior was attributed to a faulty calibration of the HSRL 1064 nm channel. The next section describes a revised calibration procedure for the 1064 nm channel that resolved this problem.

3.3 Calibration of the 1064 nm Aerosol Backscatter Profiles

In contrast to the Raman lidar measurements at 355 nm and HSRL measurements at 532 nm, no molecular backscatter measurements were made at 1064 nm because of the difficulty in measuring the extremely small molecular backscatter at this near-infrared (IR) wavelength. The lack of such a measurement at 1064 nm complicates calibration of these return signals and the computation of the aerosol backscatter profiles (Eloranta 2016). For the HSRL measurements acquired during CHARMS, the 1064 nm backscatter profiles were calibrated using measurements of the relative gains of the 1064 and 532 nm channels as well as the backscatter and optical thickness measured at 532 nm. This method also requires an estimate of the aerosol extinction Angstrom exponent between 532 and 1064 in order to account for aerosol attenuation at 1064 nm. This Angstrom exponent was obtained from coincident AErosol RObotic NETwork (AERONET) Sun photometer measurements at the SGP. Currently the 1064 nm calibration has been computed for 25 days during the CHARMS period; subsequent aerosol microphysical retrievals are restricted to these days. The same diagnostic plots were re-examined for data reprocessed using this alternative calibration method and are shown for a subset of the data in Figure 2. After revising the calibration, the backscatter color ratio (532/1064) is lower and consistent with the values observed by the LaRC airborne HSRL systems.

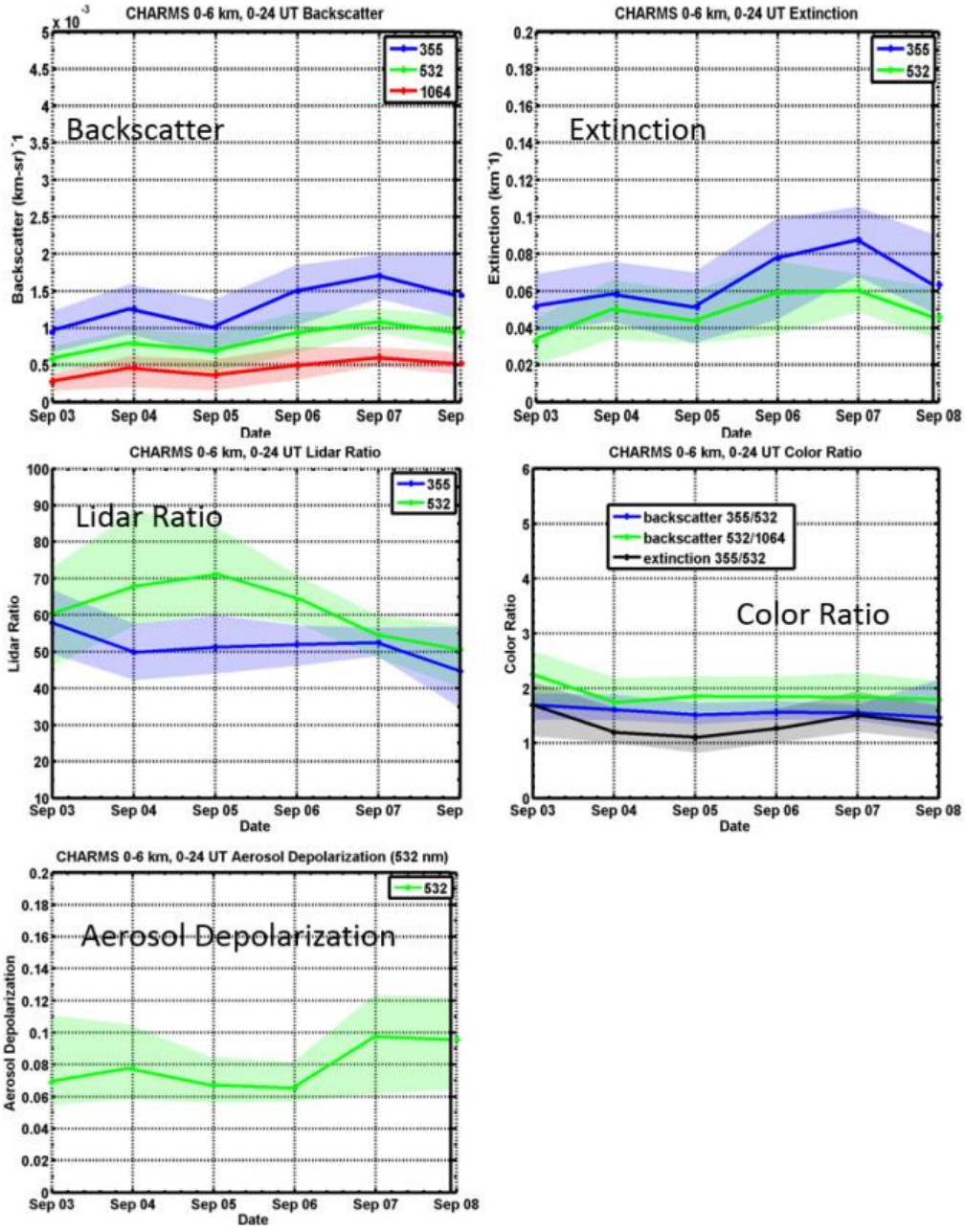

Figure 2. Same as for Figure 1 except for a subset of days (September 3-8) that use 1064 nm aerosol backscatter profiles computed using the revised calibration method.

An example of processed CHARMS data is shown in Figure 3 for September 6, 2015. Note that the backscatter and extinction color scales are the same for each wavelength. These measurements show that aerosols were concentrated below 3 km and that the aerosol vertical structure varied over this 24-hour period. These profiles also show large aerosol extinction associated with clouds at about 2.5-3 km from 13 to 17 UT and around 2-2.4 km from 18 to 21 UT.

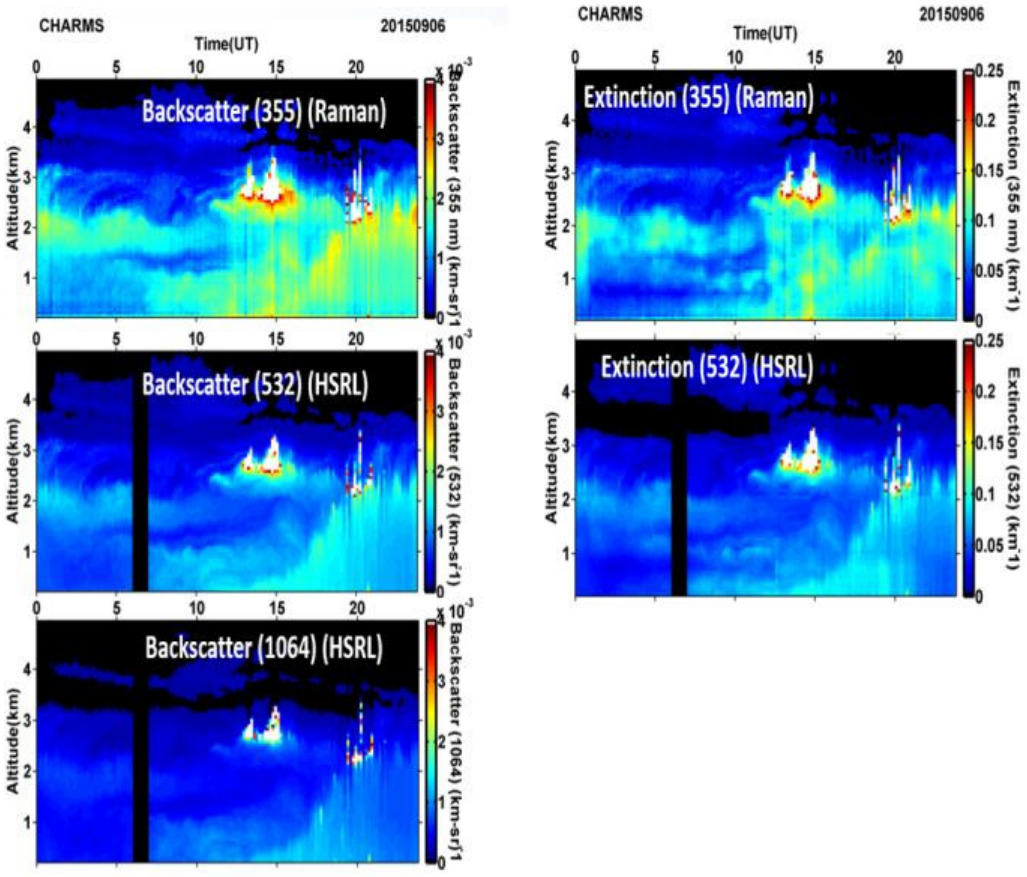

Figure 3. Example "3β+2α" data set for September 6, 2015. Temporal resolution is 10 minutes and vertical resolution is 60 m.

These CHARMS data were processed at temporal and vertical resolutions of 10 minutes and 60 meters, respectively. The processed CHARMS data set for these 25 days is available as a principal investigator (PI) product from the DOE ARM Data Archive http://iop.archive.arm.gov/arm-iop/0pi-data/?uid=FerrareR1&st=5845b00b&home=arm-archive .

4.0 Aerosol Microphysical Retrievals

The set of measurements described above was used in an automated, unsupervised 3β+2α algorithm (Müller et al. 1999, 2014; Veselovskii et al. 2002; 2004; Sawamura et al. 2017). The algorithm, which we call TiARA (Tikhonov Advanced Regularization Algorithm), uses Tikhonov regularization to derive aerosol microphysical particle parameters from multi-wavelength lidar data (Müller et al. 2014; Sawamura et al. 2017). Profiles of aerosol properties are derived from the numerical inversion of the vertically resolved particle backscatter and particle extinction coefficients. As described by Müller et al. (1999), the algorithm solves the inverse problem of deriving particle properties from lidar observations by representing the particle size distribution as a linear combination of eight logarithmically equidistant, triangular-shaped basis functions within a set of inversion windows covering particle radii from 0.03 to 8.0 µm (Müller et al. 2014; Sawamura et al. 2017). The real part of the refractive index can vary between 1.325 and 1.8 and the imaginary part can vary between 0 and 0.1. For each 3β+2α data set, the algorithm

is run nine times. In eight of these runs the extinction and backscatter coefficients are perturbed by their uncertainties in different combinations to simulate possible measurement error scenarios. The final run is performed with error-free data. Of the hundreds of thousands of solutions obtained from these nine runs for all the inversion windows and refractive indexes, the 500 with the lowest discrepancies are averaged and stored as the final solution (Müller et al. 2014; Sawamura et al. 2017). The standard deviation of the 500 best solutions provides a measure of the retrieval uncertainty. Based on sensitivity studies with synthetic data, input data with uncertainties less than about 20% provide microphysical retrieval results with satisfactory uncertainties. The 3β+2α data sets with uncertainties below 20% are used for the inversion.

Figure 4 shows an example of the retrieval results for the September 6 case shown in Figure 3. Inversions were performed at a resolution of 10 min and 120 m (increased from 60 m to reduce computation time) for data below 3 km where the lidar measurements show most of the aerosols were located. The top panels show aerosol extinction and aerosol depolarization and the panels below show the retrieved effective radius, fine-mode effective radius, fine-mode fraction, number concentration, and volume concentration. The regions shaded in purple correspond to regions where the aerosol depolarization (532 nm) is greater than 0.1 and where there was a significant presence of non-spherical particles. Because the microphysical retrievals assume the presence of spherical particles, the retrieval results in these regions are not trustworthy and so are not shown. The aerosol extinction profiles show that during much of the night (~0–7 UT), the largest aerosol extinction was located at about 2 km, likely associated with a residual layer from the previous day's mixed layer. Starting from before sunrise to early afternoon (~7–19 UT), the largest aerosol extinction was close to the surface and within the mixed layer. The aerosol extinction profiles show the rise of the mixed-layer height from near the surface to about 2.5 km by late afternoon. The retrieval results for this day show the presence of elevated concentrations of fine-mode particles above about 1 km and higher volume and number concentrations near and above the top of the mixed layer at an altitude of about 1.5–2.5 km. These higher particle concentrations may be associated with regions of higher relative humidity.

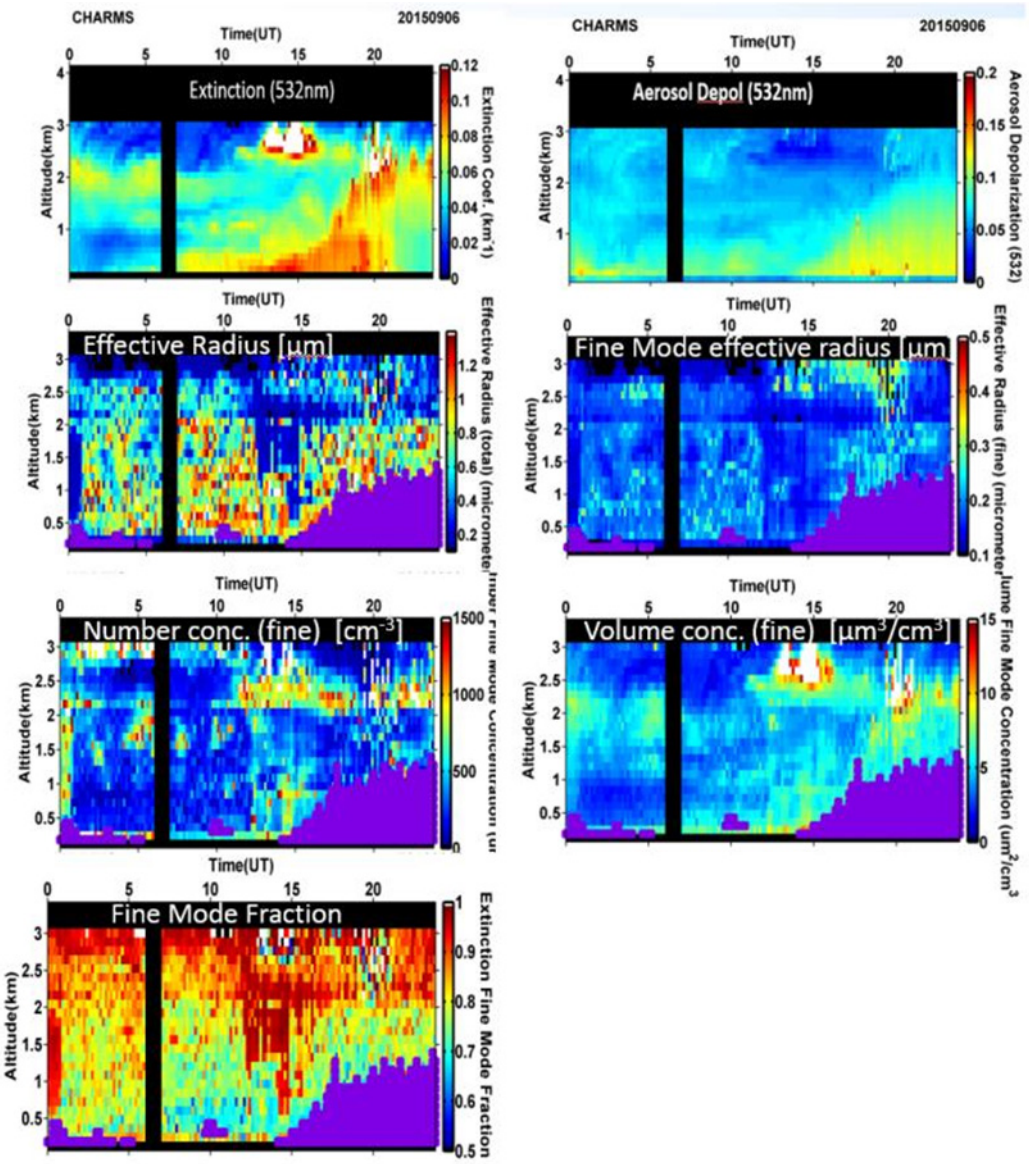

Figure 4. TiARA retrieval results for September 5, 2015. Temporal resolution is 10 minutes and vertical resolution is 120 m. Regions shaded in purple are when aerosol depolarization (532 nm) exceeds 0.1 such that non-spherical aerosols contribute significantly to aerosol backscatter and extinction.

Estimates of the uncertainties in TiARA retrievals, which are the standard operational products, have been provided by Müller et al. (2014). On average, effective radius can be retrieved to about 30% uncertainty. Most of the number density simulations have uncertainties within 100%, with uncertainty less than 70% in about half the simulations. Surface area concentration uncertainties are less than 30%. Volume concentration uncertainties are typically below 30% but can reach 50%.

Burton et al. (2016) examined the information content and sensitivity of the 3β+2α measurements for aerosol microphysical retrievals using optimal estimation methodology based on Bayes' theorem using a simplified forward model look-up table. The results indicate that the 3β+2α measurement system is underdetermined with respect to the entire suite of microphysical parameters. The study found that the

parameters retrieved with uncertainties closest to those envisioned for the NASA Aerosol-Clouds-Ecosystem (ACE) mission are associated with size distribution, particularly the total number concentration, with larger uncertainties for the complex refractive index. For this set of lidar measurements the retrievals are sensitive to particles with radii above about 50 nm and are insensitive to smaller particles (Burton et al. 2016; Chemyakin et al. 2016). Based on these retrieval studies and on microphysical retrieval results using both airborne HSRL and CHARMS data, products associated with retrievals of aerosol absorption and refractive index have unacceptably high uncertainties and so are not recommended for distribution. Recommended microphysical retrieval products include effective radius, number, surface area, volume concentrations, and fine-mode fraction.

Considering these restrictions on information provided by the 3β+2α lidar measurements, the NASA LaRC HSRL group has investigated alternative retrieval algorithms. One attempt has been to combine the TiARA and Arrange and Average (AA) algorithm described by Chemyakin et al. (2014). As an assumption, the AA uses a look-up table based on the monomodal logarithmically normal particle size distributions that cover the range of realistic ambient aerosols. Tests on synthetic data show that AA provides better results for the refractive index, in particular the real part (Chemyakin et al. 2014). The refractive index determined by AA is then used by TiARA in this experimental combined technique.

Figure 5 shows the results for the combined AA+TiARA method for the September 6 case shown in Figure 3. Results are somewhat similar, although effective radii values are significantly smaller than for the TiARA method and are closer to those derived from coincident AERONET retrievals described in the next section.

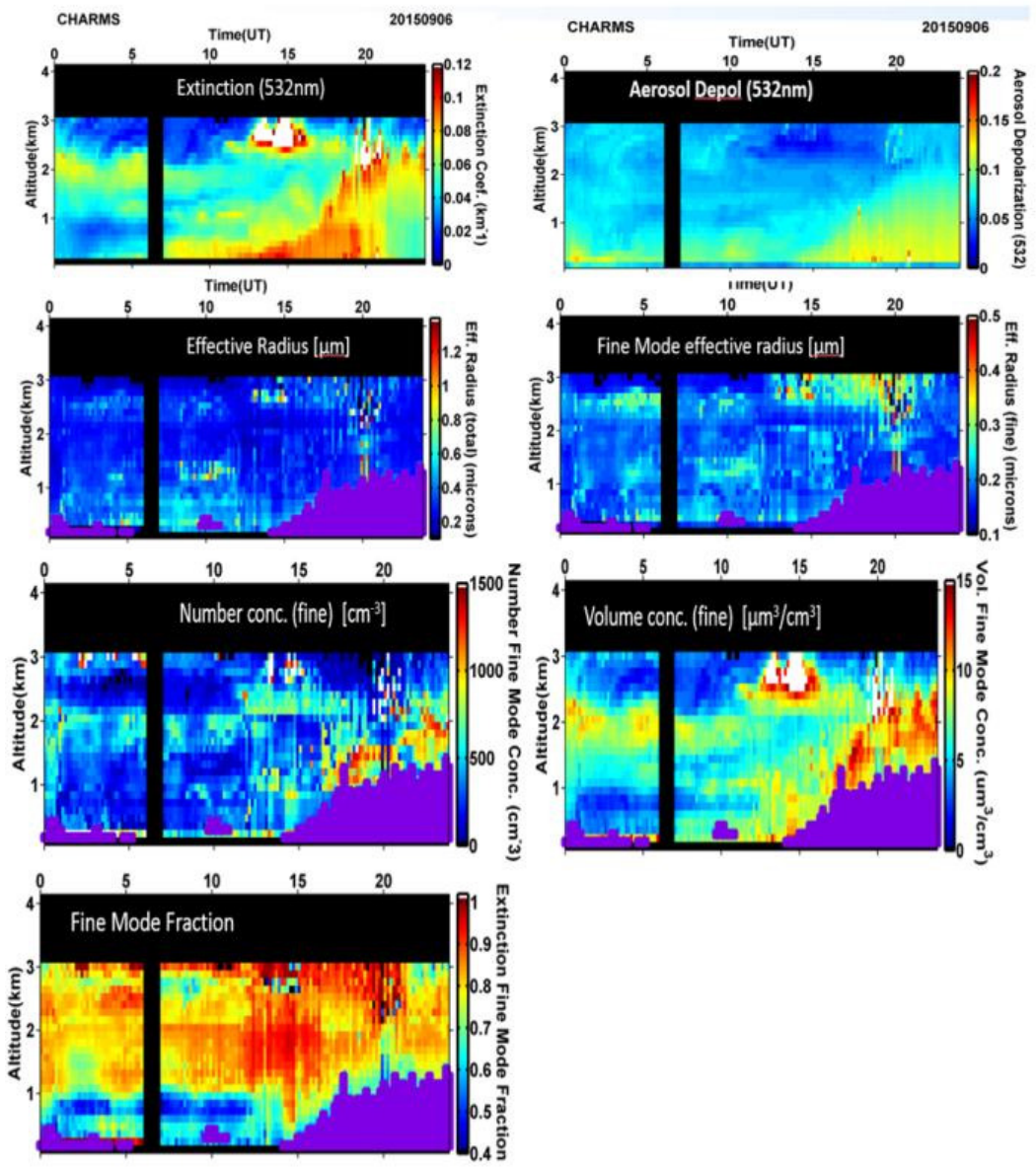

Figure 5. Same as Figure 4 except for AA+TiARA retrieval results. Temporal resolution is 10 minutes and vertical resolution is 120 m. Regions shaded in purple are when aerosol depolarization (532 nm) exceeds 0.1 such that non-spherical aerosols contribute significantly to aerosol backscatter and extinction.

5.0 Aerosol Microphysical Retrieval Comparisons with AERONET

Retrievals obtained from 3β+2α data sets measured by the NASA LaRC airborne HSRL have been compared to coincident airborne in situ data measured on the DOE Gulfstream-1 (G-1) during the DOE Two-Column Aerosol Project (TCAP) mission (Müller et al. 2014). These initial comparisons showed very good agreement among profiles of effective radius, number, surface area, and volume concentrations. Sawamura et al. (2017) performed more detailed comparisons between microphysical retrievals derived from the LaRC airborne HSRL data from the NASA Deriving Information on Surface conditions from Column and Vertically Resolved Observations Relevant to Air Quality (DISCOVER-AQ) Houston and California missions with coincident airborne in situ aerosol measurements. Figure 6 shows an example of such comparisons for profiles acquired over Houston, Texas in 2013. Sawamura et al. (2017) found that HSRL-2 airborne retrievals of ambient fine-mode aerosol surface area and volume concentrations agree with in situ measurements to within 25% and 10%, respectively, after hygroscopic growth adjustments were applied to the in situ data. Fine-mode aerosol number concentrations were within about 50% of the in situ values.

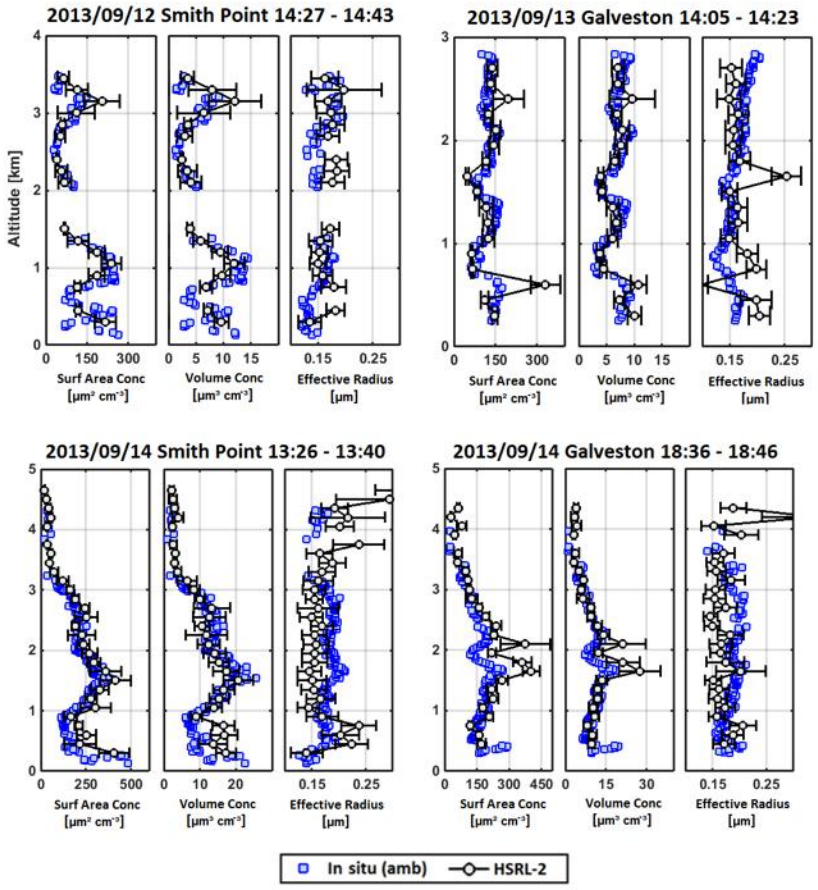

Figure 6. Comparison of TiARA aerosol retrieval results derived using NASA LaRC airborne HSRL measurements and airborne in situ data collected over the Houston, Texas region during the NASA DISCOVER-AQ mission. HSRL-2 retrievals are shown in black and in situ results are shown in blue (from Sawamura et al. 2017).

Unfortunately, coincident airborne in situ aerosol measurements were unavailable during CHARMS. Instead, the CHARMS data and column-average aerosol microphysical retrievals were compared with coincident column-average measurements and retrievals obtained from the ARM Sun photometer and processed through the NASA AERONET protocol. Although these comparisons do not provide vertically resolved results, they can provide a reference point when assessing retrieval quality. AERONET measurements and retrievals are commonly used to help assess surface (Welton et al. 2000), airborne (Shinozuka et al. 2013), and satellite (Tanre et al. 2011) aerosol remote-sensing measurements and retrievals. We acknowledge Rick Wagener of Brookhaven National Laboratory (BNL) for maintaining the SGP Sun photometer and Brent Holben of NASA's Goddard Space Flight Center (GSFC) for the AERONET analyses and retrievals.

Figure 7 shows aerosol optical depth (AOD; 355 and 532 nm) derived from the CHARMS data and compared to the AERONET level 2 measurements. CHARMS data within 10 minutes of the AERONET measurements were used in these and the following regression comparisons. The AERONET AOD values at 355 nm (wavelength of the Raman lidar) and 532 nm (wavelength of the HSRL) were obtained by logarithmically interpolating between the Sun photometer channels (340, 380, 440, 500, 640 nm). Both data sets show a significant range in AOD with values (532 nm) varying between about 0.02 and 0.6. The CHARMS data represent AOD in the column between the surface and about 8 km. Figure 7 shows excellent agreement between the CHARMS and AERONET AOD with correlations above 0.95, bias differences less than 0.03 (7%) and root-mean-square (RMS) differences less than about 0.05 (16%). Note that the CHARMS lidar provide measurements of AOD during both daytime and nighttime.

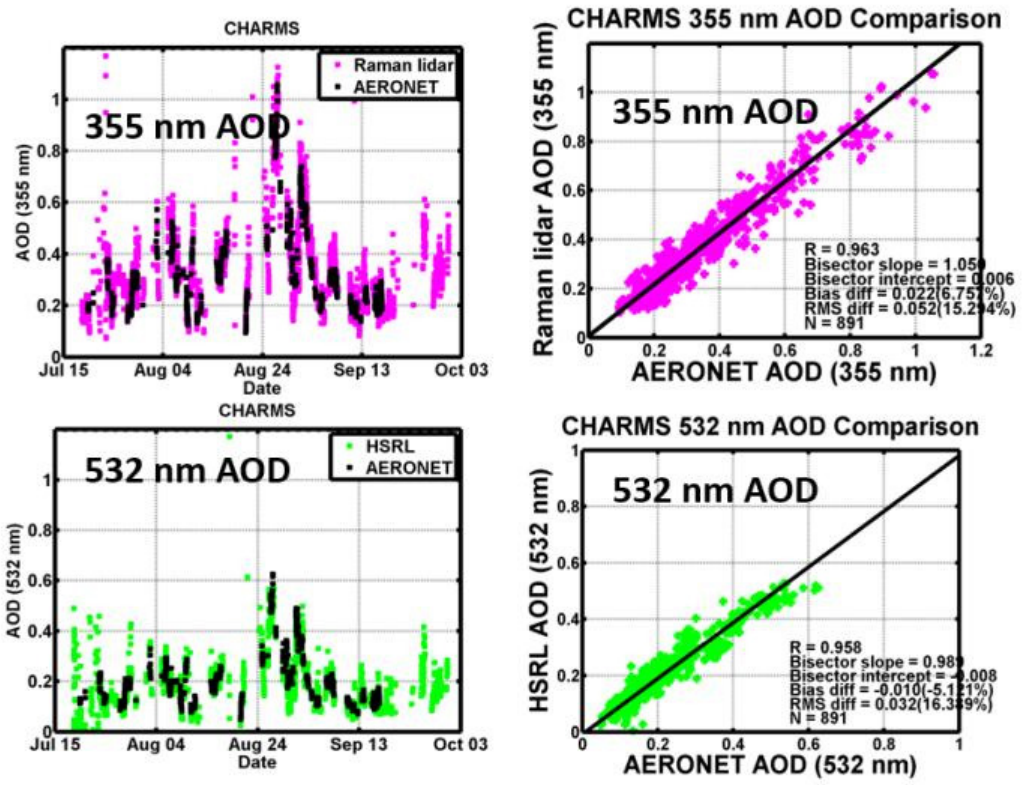

Figure 7. Comparison of aerosol optical depth (AOD) derived from the CHARMS measurements and AERONET data.

Figure 8 shows comparisons of column aerosol fine-mode AOD and column-average fine-mode fraction derived from the CHARMS (TiARA) and AERONET retrievals. The fine-mode fraction results correspond to fine-mode fraction as applied to aerosol extinction and optical thickness.

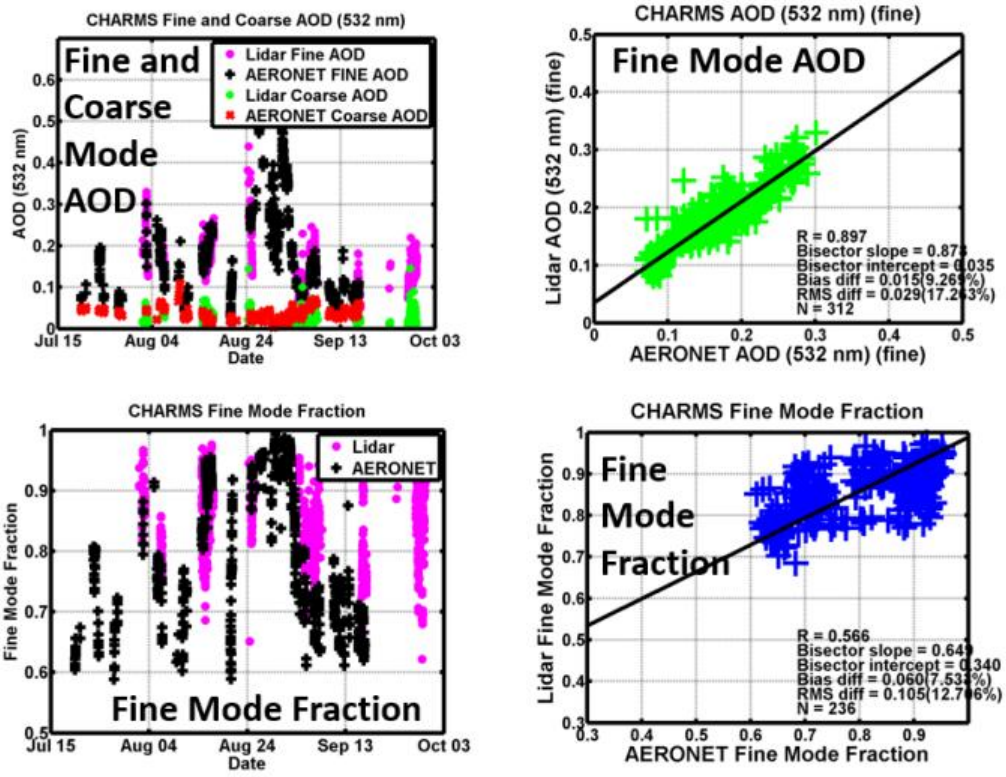

Figure 8. Comparison of fine- and coarse-mode AOD and fine-mode fraction from TiARA and AERONET SDA retrievals.

Figure 9 shows the corresponding results from the test of the combined AA+TiARA method. The AERONET retrievals of fine-mode AOD and fine-mode fraction are based on the spectral deconvolution method (SDA; O'Neill et al. 2003) described at http://aeronet.gsfc.nasa.gov/new_web/man_data.html. Note that in this figure and in those that follow, the graphs that show results as a function of date show all results, not just at the dates and times when results from both CHARMS and AERONET are available. The CHARMS retrievals of column-average fine-mode fraction represent extinction-weighted averages of the profile results. In order to avoid interference from non-spherical aerosols, these results correspond to times when the aerosol depolarization (532 nm) measured by the HSRL was less than 0.1. Figures 8 and 9 show the increase in fine-mode and total AOD during the latter part of August that may be associated with an increase in smoke over the SGP. These figures also show the decrease in total and fine-mode AOD during September, which is most likely due to the presence of coarse-mode dust; the presence of non-spherical aerosols also increased at this time. Figures 8 and 9 show a good agreement between the CHARMS and AERONET fine-mode AOD and somewhat worse agreement for fine-mode fraction.

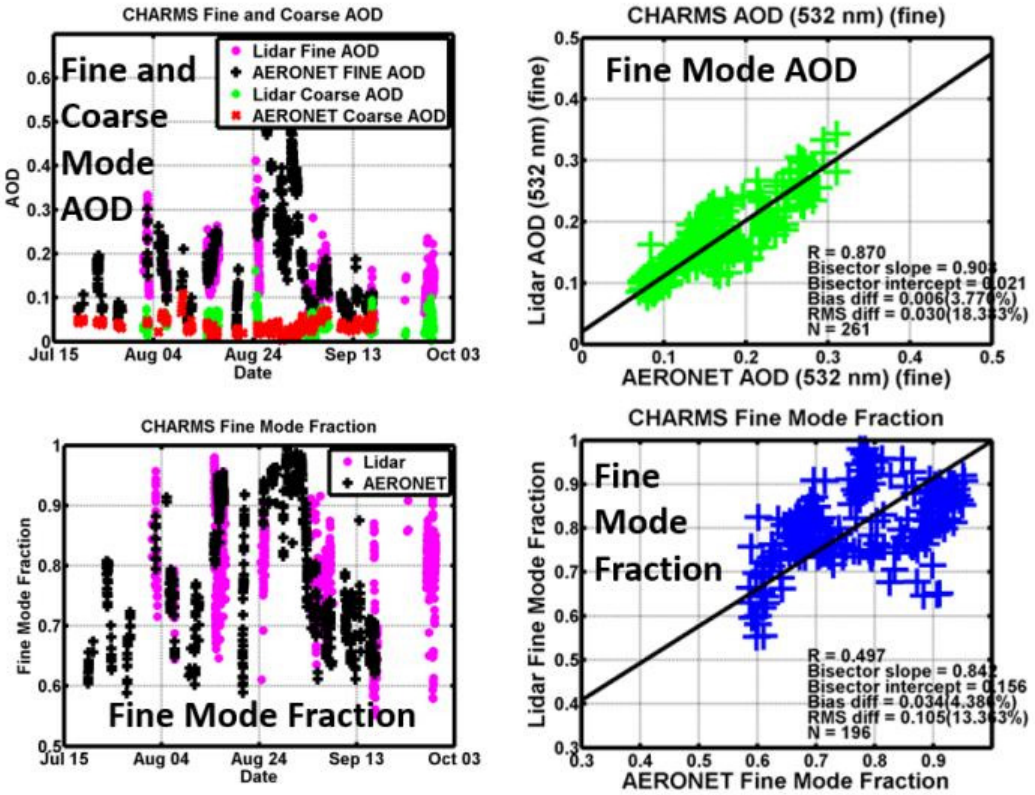

Figure 9. Same as Figure 8 except comparison of fine- and coarse-mode AOD and fine-mode fraction from AA+TiARA and AERONET SDA retrievals.

Figure 10 shows the comparison of aerosol fine-mode (top) and total (bottom) volume concentration (bottom) between the CHARMS (TiARA) and AERONET retrievals. Figure 11 shows the corresponding results from the test of the combined AA+TiARA method. A description of the AERONET retrievals used to derive these results can be found at http://aeronet.gsfc.nasa.gov/new_web/Documents/inversions.pdf.

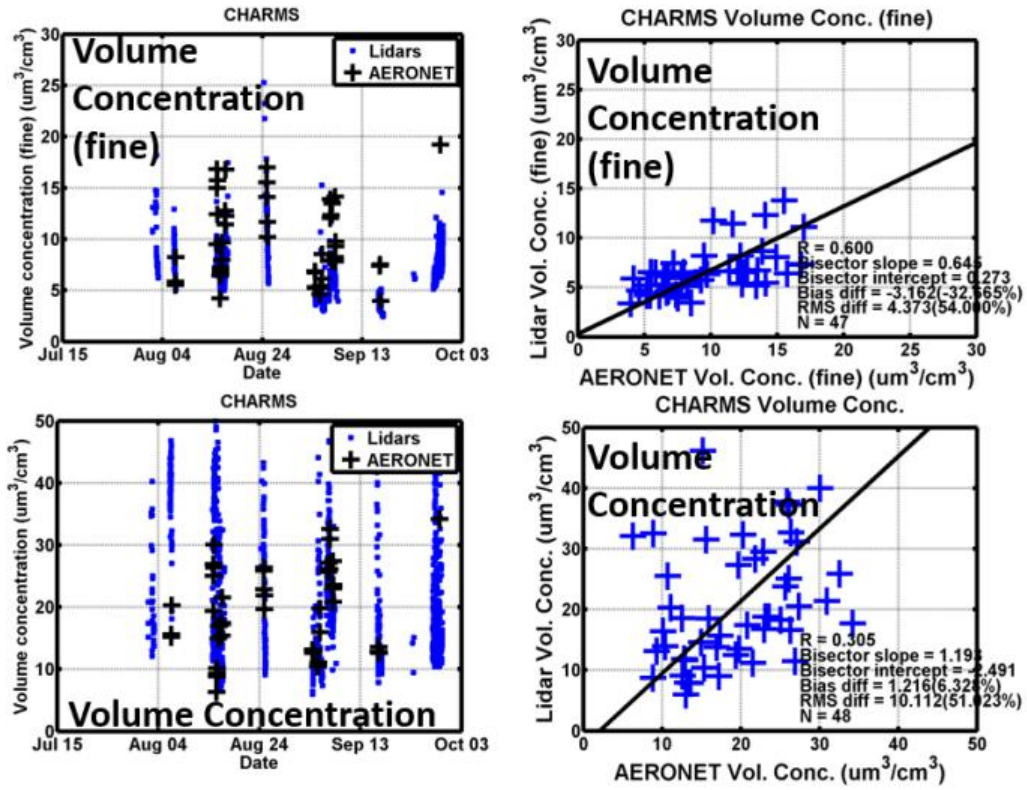

Figure 10. Comparison of fine (top) and total (bottom) volume concentrations from TiARA and AERONET retrievals.

These retrievals are also described by Dubovik et al. (2000) and Dubovik and King (2000). AERONET retrievals produce volume size distributions integrated on the atmospheric column (i.e., $\mu m^3/cm^2$). In order to compare the AERONET retrievals with the CHARMS retrievals, the depth below which 90% of the AOD was located as determined from the CHARMS HSRL 532 nm extinction profiles was used to convert the AERONET column volume concentrations to volume concentration units (i.e., $\mu m^3/cm^3$). The CHARMS retrievals of concentrations represent extinction-weighted averages of the profile results. Figures 10 and 11 show reasonable agreement between the AERONET and CHARMS values, with better agreement for fine-model volume concentration than total volume concentration.

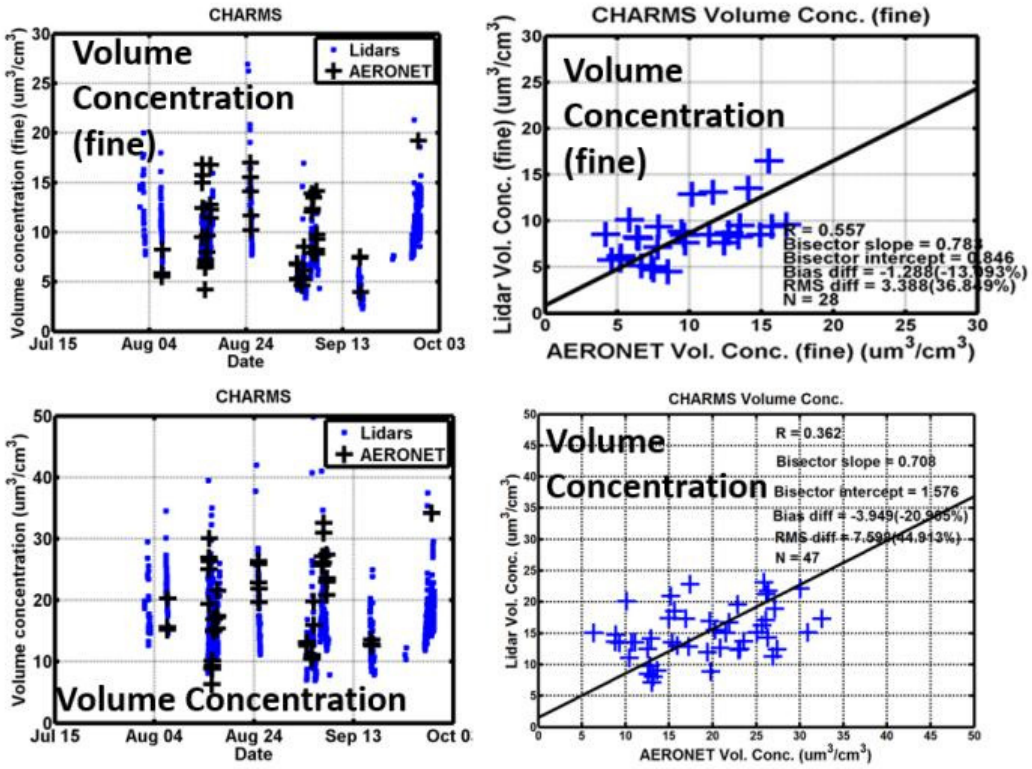

Figure 11. Same as Figure 10 except for comparison of fine (top) and total (bottom) volume concentrations from AA+TiARA and AERONET retrievals.

Figure 12 shows a comparison of aerosol fine (top) and total (bottom) effective radius between the CHARMS (TiARA) and AERONET retrievals. Figure 13 shows the corresponding results from the test of the combined AA+TiARA method. The CHARMS retrievals of effective radii represent extinction-weighted averages of the profile results. The CHARMS values of fine-mode effective radii appear to span a larger range than the AERONET values. This is even more pronounced in the total effective radius comparisons. Here the AA+TiARA method appears to provide total effective radii more consistent with the values derived from the AERONET data set.

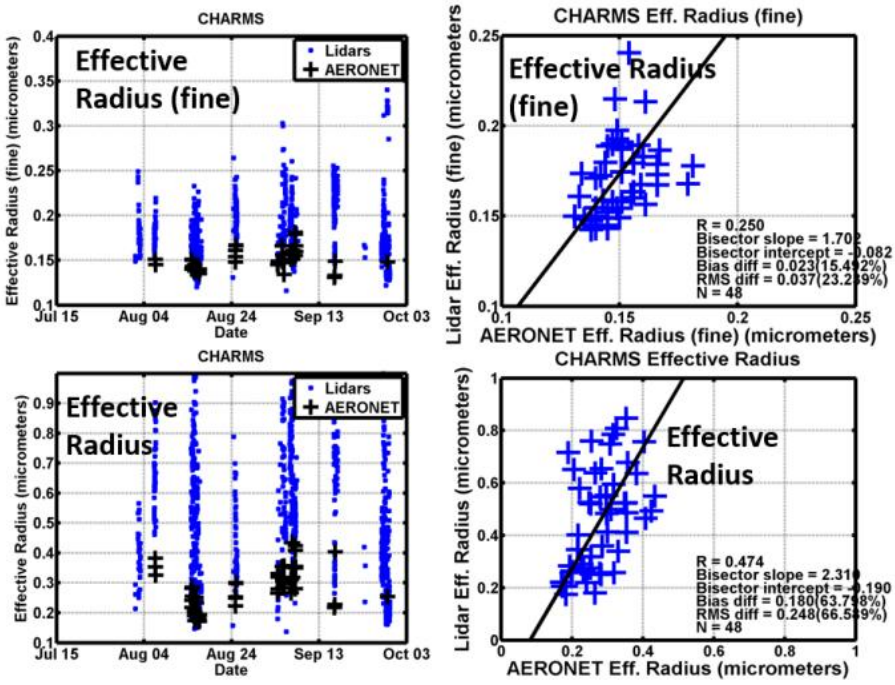

Figure 12. Comparison of fine (top) and total (bottom) effective radii from TiARA and AERONET retrievals.

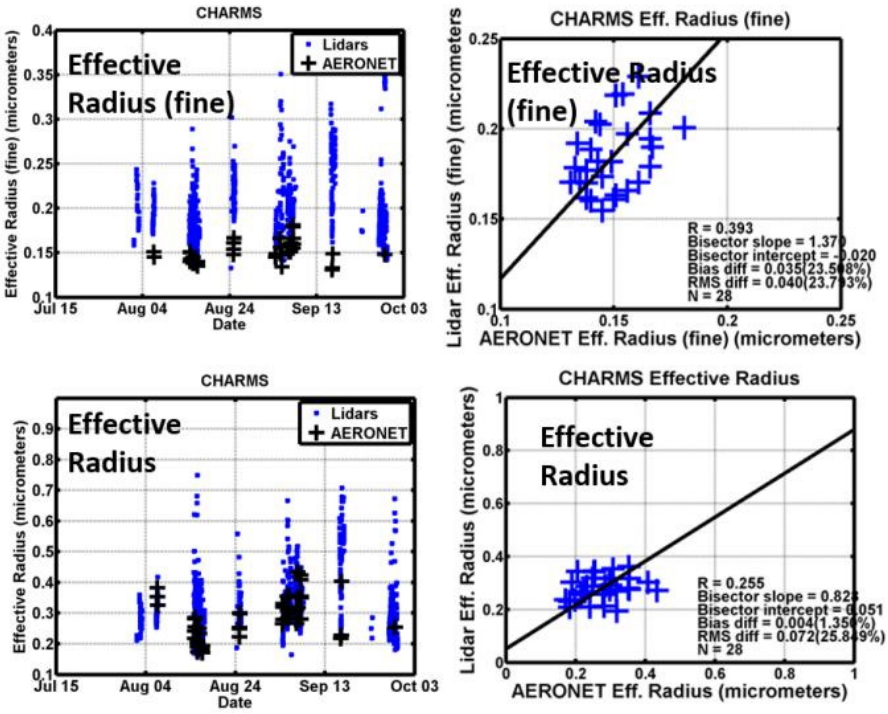

Figure 13. Same as Figure 12 except for comparison of fine (top) and total (bottom) effective radii from AA+TiARA and AERONET retrievals.

6.0 Summary and Outlook

CHARMS provided an opportunity to explore aerosol microphysical retrievals with data collected by ground-based lidars supported by the DOE ARM Facility. CHARMS was unique in that it provided extensive (24/7) data sets collected by ground-based lidars over many days in contrast to a few episodic measurements. CHARMS demonstrated that the combination of the SGP Raman lidar and the UW HSRL can collect a multi-wavelength lidar data set suitable for retrieving profiles of aerosol microphysical properties such as fine-mode fraction, particle concentration, and effective radius. CHARMS measurements of AOD compare well with simultaneous AERONET retrievals of AOD. For cases when the contribution by non-spherical aerosols to aerosol backscatter and extinction is small, the resulting column-average retrievals of aerosol fine-mode fraction, particle concentration, and effective radii compare favorably with corresponding column-average retrievals from AERONET.

The CHARMS data collected during July-September, 2015 exhibited a somewhat surprisingly large number of days with significant amounts of non-spherical aerosols as revealed by the aerosol depolarization values greater than 0.1. Initial analyses suggest that these non-spherical aerosols are likely dust, are concentrated within the mixed layer, and contain higher fractions of coarse-mode aerosols. Although the microphysical retrievals are not performed in the presence of non-spherical aerosols, the CHARMS data still provided more frequent retrievals than AERONET (CHARMS provides retrievals during both day and night and below clouds) and provided vertical information that is unavailable from AERONET.

A significant challenge in processing the CHARMS data has been the production of calibrated 1064 nm aerosol backscatter profiles. Because molecular scattering is very weak at 1064 nm, unlike 355 or 532 nm, it is currently not feasible to measure molecular scattering at 1064 nm using Raman or HSRL techniques. Consequently, the lack of a separate measurement of molecular scattering at 1064 nm can complicate the calibration of this channel and introduce greater uncertainty in the aerosol backscatter profiles. This was particularly relevant for the UW HSRL, which had only recently been modified to permit measurement of the 1064 nm signal during daytime as well as nighttime operations. Further optimization of this system (e.g., to reduce the susceptibility of this channel to changes in alignment) would likely make calibration and processing easier and reduce backscatter profile uncertainties. After CHARMS, the RLID was modified to reduce misalignments and signal fluctuations and the performance was improved; we anticipate these changes would also improve the quality of aerosol microphysical retrievals from any possible future CHARMS-like measurements.

The NASA LaRC HSRL group is continuing to develop and test multi-wavelength lidar aerosol microphysical retrieval algorithms. In addition to the TiARA and AA methods discussed earlier, an alternative aerosol retrieval scheme based on Optimal Estimation (OE) is also under development. The TiARA approach solves for aerosol size distributions in the size and composition parameter space (r_{min}, r_{max}, real and imaginary refractive index) using Tikhonov regularization and then selects physically and mathematically meaningful solutions from hundreds of thousand retrievals. In contrast, the OE method solves for all related aerosol microphysical parameters (number concentrations, particle size distribution, real and imaginary part of refractive indices) simultaneously in a maximum-likelihood sense by fitting the observed data. The OE method has been widely used in the passive remote sensing community (e.g., Liu et al. 2009) because it provides a more physically based mechanism for introducing vertical correlations in the background covariance matrix. OE also provides error estimates of the retrieved parameters and provides a mechanism for including knowledge of vertical correlations in the profile retrieval.

Perhaps more importantly, the OE method provides a methodology to more easily combine the lidar data with passive remote-sensing data. As discussed earlier, the lidar data alone are insufficient to accurately retrieve aerosol absorption and refractive index in addition to particle size and concentration. Additional data, from airborne passive sensors such as a multi-wavelength, multi-angle polarimeter can provide powerful constraints to allow profile retrievals of aerosol absorption and refractive index for airborne HSRL data. Similarly, additional information from ground-based passive sensors, such as from AERONET Sun photometer and/or MFRSR direct/diffuse measurements, can also provide similar constraints for retrievals that use ground-based lidar measurements.

The NASA LaRC HSRL group is developing an OE retrieval methodology that combines multi-wavelength 3β+2α lidar data with polarimeter data for these aerosol retrievals. Initial studies using airborne HSRL data from the DOE TCAP mission show that the OE retrievals that use only 3β+2α lidar data provide results similar to the TiARA and AA+TiARA retrievals (Liu et al. 2016) for size distribution and concentration parameters. Likewise, initial studies of OE retrievals that use only coincident airborne polarimeter data from TCAP produce column-average aerosol properties that are consistent with the lidar measurements and retrievals and also produce realistic column-average aerosol absorption and refractive indices. We are cautiously optimistic that OE retrievals that incorporate data from both multi-wavelength lidars and passive sensors (e.g., polarimeters, Sun photometers, MFRSR) will provide profiles of aerosol absorption and refractive index in additional to particle size and concentration. Until such OE retrieval algorithms are available, we recommend that the NASA LaRC HSRL group process the data from any future CHARMS-like missions using the TiARA retrieval described here; these results can be released as a PI product. We have already released the CHARMS 3β+2α data sets as a PI product (http://iop.archive.arm.gov/arm-iop/0pi-data/?uid=FerrareR1&st=5845b00b&home=arm-archive) and are working toward releasing the TiARA retrieval results from CHARMS.

7.0 References

Burton, SP, RA Ferrare, CA Hostetler, JW Hair, RR Rogers, MD Obland, CF Butler, AL Cook, DB Harper, and KD Froyd. 2012. "Aerosol classification using airborne High Spectral Resolution Lidar measurements–methodology and examples." *Atmospheric Measurement Techniques* 5(1): 73-98, doi:10.5194/amt-5-73-2012.

Burton, SP, E Chemyakin, X Liu, K Knobelspiesse, S Stamnes, P Sawamura, RH Moore, CA Hostetler, and RA Ferrare. 2016. "Information content and sensitivity of the 3 beta+2 alpha lidar measurement system for aerosol microphysical retrievals." *Atmospheric Measurement Techniques* 9(11): 5555-5574, doi:10.5194/amt-9-5555-2016.

Chemyakin, E, D Muller, S Burton, A Kolgotin, C Hostetler, and R Ferrare .2014. "Arrange and average algorithm for the retrieval of aerosol parameters from multiwavelength high-spectral-resolution lidar/Raman lidar data." *Applied Optics* 53(31): 7252-7266, doi:10.1364/AO.53.007252.

Chemyakin, E, S Burton, A Kolgotin, D Muller, C Hostetler, and R Ferrare. 2016. "Retrieval of aerosol parameters from multiwavelength lidar: investigation of the underlying inverse mathematical problem." *Applied Optics* 55(9): 2188-2202, doi:10.1364/Ao.55.002188.

Dubovik, O, and MD King. 2000. "A flexible inversion algorithm for retrieval of aerosol optical properties from Sun and sky radiance measurements." *Journal of Geophysical Research–Atmospheres* 105(D16): 20673-20696, doi:10.1029/2000JD900282.

Dubovik, O, A Smirnov, BN Holben, MD King, YJ Kaufman, TF Eck, and I Slutsker. 2000. "Accuracy assessments of aerosol optical properties retrieved from Aerosol Robotic Network (AERONET) Sun and sky radiance measurements." *Journal of Geophysical Research–Atmospheres* 105(D8): 9791-9806, doi:10.1029/2000JD900040.

Eloranta, EW. 2014. "High spectral resolution lidar measurements of atmospheric extinction: Progress and challenges." *IEEE Aerospace Conference*, doi:10.1109/AERO.2014.6836214.

Eloranta, EW. 2016. "CHARMS-Calibration of the 1064 nm HSRL Channel." U.S. Department of Energy Atmospheric Systems Research 7th Science Team Meeting, May 2-5, Vienna, VA.

Goldsmith, JEM, FH Blair, SE Bisson, and DD Turner. 1998. "Turn-key Raman lidar for profiling atmospheric water vapor, clouds, and aerosols." *Applied Optics* 37(21): 4979-4990, doi:10.1364/Ao.37.004979.

Grund, CJ, and EW. Eloranta. 1991. "University-of-Wisconsin High Spectral Resolution Lidar." *Optical Engineering* 30(1): 6-12, doi:101117/12.55766.

Liu, X, S Stamnes, RA Ferrare, C Hostetler, S Burton, E Chemyakin, P Sawamura, D Müller, and B Cairns. 2016. "Development of a combined lidar–polarimeter inversion algorithm for retrieving aerosol." AGU, Fall General Assembly 2016, abstract A54E-06.

Liu, X, DK Zhou, AM Larar, WL Smith, P Schluessel, SM Newman, JP Taylor, and W Wu. 2009. "Retrieval of atmospheric profiles and cloud properties from IASI spectra using super-channels." *Atmospheric Chemistry and Physics* 9(23): 9121-9142, doi:10.5194/acp-9-9121-2009.

Müller, D, CA Hostetler, RA Ferrare, SP Burton, E Chemyakin, A Kolgotin, JW Hair, AL Cook, DB Harper, RR Rogers, RW Hare, CS Cleckner, MD Obland, J Tomlinson, LK Berg, and B Schmid. 2014. "Airborne Multiwavelength High Spectral Resolution Lidar (HSRL-2) observations during TCAP 2012: Vertical profiles of optical and microphysical properties of a smoke/urban haze plume over the northeastern coast of the US." *Atmospheric Measurement Techniques* 7(10): 3487-3496, doi:10.5194/amt-7-3487-2014.

Müller, D, U Wandinger, and A Ansmann. 1999. "Microphysical particle parameters from extinction and backscatter lidar data by inversion with regularization: theory." Applied Optics 38(12): 2346-2357, doi:10.1364/AO.38.002346.

O'Neill, NT, TF Eck, A Smirnov, BN Holben, and S Thulasiraman. 2003. "Spectral discrimination of coarse and fine mode optical depth." *Journal of Geophysical Research–Atmospheres* 108(D17), doi:1029/2002JD002975.

Piironen, P, and EW Eloranta. 1994. "Demonstration of a high-spectral-resolution lidar based on an iodine absorption filter." *Optics Letters* 19(3): 234-236, doi:10.1364/OL.19.000234.

Sawamura, P, RH Moore, SP Burton, E Chemyakin, D Muller, A Kolgotin, RA Ferrare, CA Hostetler, LD Ziemba, AJ Beyersdorf, and BE Anderson. 2017. "HSRL-2 aerosol optical measurements and microphysical retrievals vs. airborne in situ measurements during DISCOVER-AQ 2013: An intercomparison study." *Atmospheric Chemistry and Physics Discussions* 17(11):7229-7243, doi:10.5194/acp-2016-1164.

Schmid, B, CJ Flynn, RK Newsom, DD Turner, RA Ferrare, MF Clayton, E Andrews, JA Ogren, RR Johnson, PB Russell, WJ Gore, and R Dominguez. 2009. "Validation of aerosol extinction and water vapor profiles from routine Atmospheric Radiation Measurement Program Climate Research Facility measurements." *Journal of Geophysical Research–Atmospheres* 114(D22), doi:10.1029/2009JD012682.

Shinozuka, Y, RR Johnson, CJ Flynn, PB Russell, B Schmid, J Redemann, SE Dunagan, CD Kluzek, JM Hubbe, M Segal-Rosenheimer, JM Livingston, TF Eck, R Wagener, L Gregory, D Chand, LK Berg, RR Rogers, RA Ferrare, JW Hair, CA Histetler, and SP Burton. 2013. "Hyperspectral aerosol optical depths from TCAP flights." *Journal of Geophysical Research–Atmospheres* 118(21): 12180-12194, doi:10.1002/2013JD020596.

Tanre, D, FM Breon, JL Deuze, O Dubovik, F Ducos, P Francois, P Goloub, M Herman, A Lifermann, and F Waquet. 2011. "Remote sensing of aerosols by using polarized, directional and spectral measurements within the A-Train: the PARASOL mission." *Atmospheric Measurement Techniques* 4(7): 1383-1395, doi:10.5194/amt-4-1383-2011.

Thorsen, TJ, Q Fu, RK Newsom, DD Turner, and JM Comstock. 2015. "Automated retrieval of cloud and aerosol properties from the ARM Raman lidar. Part I: Feature detection." *Journal of Atmospheric and Oceanic Technology* 32(11): 1977-1998, doi:10.1175/JTECH-D-14-00150.1.

Thorsen, TJ, and Q Fu. 2015. "Automated retrieval of cloud and aerosol properties from the ARM Raman lidar. Part II: Extinction." *Journal of Atmospheric and Oceanic Technology* 32(11): 1999-2023, doi:10.1175/JTECH-D-14-00178.1.

Turner, DD, RA Ferrare, LAH Brasseur, and WF Feltz. 2002. "Automated retrievals of water vapor and aerosol profiles from an operational Raman lidar." *Journal of Atmospheric and Oceanic Technology* 19(1): 37-50, doi:10.1175/1520-0426(2002)019<0037:AROWVA>2.0.CO;2.

Turner, DD, and JEM Goldsmith. 1999. "Twenty-four-hour Raman lidar water vapor measurements during the Atmospheric Radiation Measurement Program's 1996 and 1997 water vapor intensive observation periods." *Journal of Atmospheric and Oceanic Technology* 16(8): 1062-1076, doi:10.1175/1520-0426(1999)016<1062:TFHRLW>2.0.Co;2.

Veselovskii, I, A Kolgotin, V Griaznov, D Muller, K Franke, and DN Whiteman. 2004. "Inversion of multiwavelength Raman lidar data for retrieval of bimodal aerosol size distribution." *Applied Optics* 43(5): 1180-1195, doi:10.1364/AO.43.001180.

Veselovskii, I, A Kolgotin, V Griaznov, D Muller, U Wandinger, and DN Whiteman. 2002. ""Inversion with regularization for the retrieval of tropospheric aerosol parameters from multiwavelength lidar sounding." *Applied Optics* 41(18): 3685-3699, doi:10.1364/AO.41.003685.

Welton, EJ, KJ Voss, HR Gordon, H Maring, A Smirnov, B Holben, B Schmid, JM Livingston, PB Russell, PA Durkee, P Formenti, and MO Andreae. 2000. "Ground-based lidar measurements of aerosols during ACE-2: Instrument description, results, and comparisons with other ground-based and airborne measurements." *Tellus B* 52(2): 636-651, doi:10.1034/j.1600-0889.2000.00025.xs.


ARM
CLIMATE RESEARCH FACILITY

www.arm.gov


U.S. DEPARTMENT OF
ENERGY
Office of Science